Physics of Atomic Nuclei, Vol. 57, No. 9, 1994, pp. 1559 - 1564. From Yadernaya Fizika, Vol. 57, No. 9, 1994, pp. 1632 - 1637.

$\bar{N}N$ INTERACTION (ANNIHILATION AND SCATTERING)

Exclusive Reactions at High Q^2 and Polarization Phenomena*

F. Myhrer[1)]

Abstract – Arguments are presented for the expected high-energy and large-scattering angle behavior of $\pi N \longrightarrow \pi N$ scattering and the $\bar{p}p \longrightarrow \pi\pi$ reaction cross sections. The annihilation reaction has close to maximal asymmetry (≈ 1) for $p_{lab} \lesssim 2.2$ GeV/c, a feature that can be understood via a simple relation between helicity–flip and helicity–nonflip partial-wave amplitudes. At higher energies and large Q^2, where perturbative QCD becomes applicable, this large asymmetry will start to oscillate with increasing energy for fixed (90°) angle. This is due to the energy dependence of a QCD phase of the independent quark–quark (Landshoff) scattering amplitude at high but not asymptotic energies. A consequence is that, even if helicity is conserved at the quark level ($m_q = 0$ MeV), helicity does not have to be conserved on the hadronic level. The implications for spin observables in pp elastic scattering will be discussed and it will be argued that these QCD phenomena are easier to examine theoretically in the $\pi N \longrightarrow \pi N$ scattering and/or in the crossed-channel reaction $\bar{p}p \longrightarrow \pi\pi$.

1. INTRODUCTION

For proton–proton elastic scattering at high-momentum transfer (High Q^2) at $\theta = 90°$, the following observations are of importance in the discussion below:

(1) The energy behavior of the differential cross section at $\theta = 90°$ for exclusive hadronic reactions is approximately described by the simple perturbative QCD (pQCD) counting rules [1]. For example, the "short distance" QCD proton–proton elastic scattering amplitude M_{SD} at high Q^2 and $\theta = 90°$ changes with energy as

$$M_{SD} \sim Q^{-8} \sim s^{-4},$$

where s equals the square of the center-of-mass energy. This implies that the differential cross section $d\sigma/dt$ decreases with increasing energy as s^{-10}, or that the "scaled" cross section

$$s^{10}\frac{d\sigma}{dt}\bigg|_{90°} \approx \text{constant}.$$

However, the measured "scaled" cross section is not quite constant; it shows oscillations with $\ln(s)$ as shown in Fig. 1.

(2) The measured polarization

$$A_{0n} = \frac{d\sigma(\uparrow) - d\sigma(\downarrow)}{d\sigma(\uparrow) + d\sigma(\downarrow)}$$

increases with increasing Q^2 [2]. This behavior is unexpected in pQCD due to the following argument: for massless quarks, the quark–gluon interaction cannot flip the spin of the quark, meaning quark helicity is conserved in pQCD. Therefore, for exclusive hadronic reactions at sufficiently high energy and high Q^2, we then infer that the hadron helicity is also conserved, i.e., we expect $A_{0n} \longrightarrow 0$ as $Q^2 \longrightarrow \infty$.

Based on the observed oscillations of the "scaled" cross section and the measured Q^2 behavior of A_{0n}, we could question if we have reached the high Q^2 region where pQCD arguments are valid. However, as will be discussed here, these observations might be consistent with pQCD expectations. We will argue that some possible QCD processes contributing to the high Q^2 exclusive hadronic reactions have been overlooked by many when "QCD phenomenology" predictions for these reactions have been made.

In the following, we will discuss QCD predictions for the following reactions: (1) pp elastic scattering ($\theta = 90°$), (2) πp elastic scattering at $\theta = 90°$, and (3) $\bar{p}p \longrightarrow$ two pseudoscalar mesons at $\theta = 90°$. In the last reaction, the final-state pairs of mesons could be ${}^+K^-$, $\pi^+\pi^-$, $\pi^0\pi^0$, $\pi^0\eta$, and $\eta\eta$. (The annihilation reactions leading to the

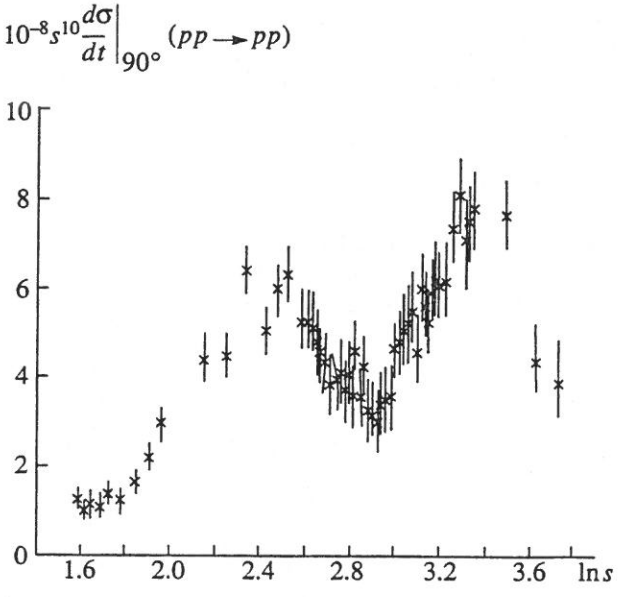

Fig. 1. The elastic pp cross section at 90° scaled by s^{10} as a function of energy. Figure taken from the review of Sivers *et al.* [1].

* This article was submitted by the author in English.

[1)] Department of Physics and Astronomy, University of South Carolina, Columbia, SC 29208, USA

1063-7788/94/5709-1559$10.00 © 1994 МАИК Наука/Interperiodica Publishing

latter three final states are presently being analyzed by the E760 collaboration at Fermilab [3].) The two first annihilation reactions are interesting because (almost) maximal "polarization" ($A_{0n} \approx +1$) has been observed for $p_{lab} \approx 2$ GeV/c [4 - 6]. As we increase the energy (or s), "short distance" QCD arguments mentioned above say $A_{0n} \longrightarrow 0$ as $s \longrightarrow \infty$. The intriguing possibility that triggered this investigation is that we could use A_{0n} of these two annihilation reactions to investigate experimentally at what energy "QCD arguments" become applicable for exclusive hadronic reactions.

We consider the few-GeV/c energy region to be a transition region between the low-energy region $p_{lab} \lesssim 1$ GeV/c described by effective meson–baryon interactions, where a coupled-channels method with the explicit enumeration of possible hadronic channels may be a useful theoretical framework [7, 8], and the high-energy regime, where perturbative QCD calculations are valid. First, we will present a possible mechanism why A_{0n} is maximal for the annihilation reactions $\bar{p}p \longrightarrow K^-K^+$ or $\bar{p}p \longrightarrow \pi^-\pi^+$ in this energy transition region ($p_{lab} \approx 2$ GeV/c). Then, we will discuss the expected energy behavior of these reactions at high Q^2 and propose some experiments to look for these predicted phenomena.

2. A DIFFRACTION MODEL ANALYSIS FOR THE TRANSITION REGION

The annihilation reaction $\bar{p}p \longrightarrow \pi^-\pi^+$ and πN elastic scattering are, in principle, described by the same two helicity amplitudes, the spin–non-flip f_{++} and the spin–flip f_{+-}. As stated above the experimentally-observed asymmetries A_{0n} in the annihilation reaction $\bar{p}p \longrightarrow K^-K^+$ seem to reach the maximal possible value of +1 over wide ranges of angles and p_{lab} between about 1 GeV/c and 2.2 GeV/c [4 - 6]. The reaction $\bar{p}p \longrightarrow \pi^-\pi^+$ has a very large A_{0n} for $p_{lab} \gtrsim 1.5$ GeV/c. These remarkable features call for a simple explanation. This explanation must simultaneously account for the following aspects of the observed differential cross sections: the $d\sigma/d\Omega$ for the final $\pi^-\pi^+$ reaction shows pronounced oscillations, whereas that of the final K^-K^+ reaction has a strong forward peak and a smooth backward plateau. Early model analyses of the strong angular oscillations seen in $d\sigma/d\Omega$ for $\bar{p}p \longrightarrow \pi^-\pi^+$ lead to the speculation of the existence of possible $J = 3$, 4, and 5 meson resonances [9]. However, a weak point in this analysis was the assumption that one partial wave dominates at each energy. A recent partial wave analysis based on dispersion relation theory of the $\bar{p}p \longrightarrow \pi^-\pi^+$ reaction is not incompatible with "resonance activity" in some partial waves [10]. Our illustrative "geometrical" analysis [11] does not require any explicit meson resonances and will reproduce, in a natural way, the observed behavior of A_{0n} and $d\sigma/d\Omega$.

In terms of the two helicity amplitudes, the cross section and the asymmetry are given as

$$d\sigma/d\Omega = |f_{++}|^2 + |f_{+-}|^2$$

and

$$A_{0n} = 2\,\mathrm{Im}(f^*_{++}f_{+-})/(d\sigma/d\Omega)\,. \tag{1}$$

The partial wave expansion defines the relevant amplitudes T^J_+ and T^J_-:

$$f_{++} = \frac{1}{p}\sum_{J=0}^{\infty}(J+\frac{1}{2})\,T^J_+ P_J(\cos\theta) \tag{2}$$

and

$$f_{+-} = \frac{1}{p}\sum_{J=0}^{\infty}(J+\frac{1}{2})/\sqrt{J(J+1)}\,T^J_- P'_J(\cos\theta)\sin\theta. \tag{3}$$

Conservation of parity and angular momentum implies that only tensor-coupled $\bar{N}N$ partial waves ($J = L \pm 1$) contribute to this annihilation reaction. Since we expect that the helicity flip amplitude is most effective at the interaction surface, we assume that T^J_- is given by the derivative of T^J_+ with respect to the impact parameter b:

$$T^J_- = \mathrm{const}\,\partial T^J_+/\partial b. \tag{4}$$

Then, using $J \approx pb$, we find the basic "differential" relation

$$T^J_- \propto \Delta T^J_+/\Delta J \tag{5}$$

or

$$\frac{J+\frac{1}{2}}{\sqrt{J(J+1)}}T^J_- = \frac{1}{\beta}(T^{J-1}_+ - T^{J+1}_+)\,, \tag{6}$$

where β is assumed to be a complex constant parameter. (We can show in a DWBA-type calculation that β is almost constant as a function of θ [11].) This assumption leads to

$$f_{+-} = -\frac{1}{\beta}f_{++}\sin\theta, \tag{7}$$

and consequently, from equation (1),

$$A_{0n} = \frac{2\,\mathrm{Im}\,\beta}{|\beta|^2 + \sin^2\theta}\sin\theta. \tag{8}$$

If the parameter β is imaginary, then A_{0n} of equation (8) will be larger than 0.9 over a very wide angular range ($|\cos\theta| \sim 0.8$), whereas $d\sigma/d\Omega$ may have a significantly stronger angular dependence, determined by $f_{++}(\theta)$ [11]. Since so many competing annihilation channels are open at the energies under discussion, we assume, as an explicit model example, that the amplitudes are given by "classical" grey- or black-sphere amplitudes

$$T^J_+ = \begin{cases} B\exp(-aJ) & (J \le J_{max}) \\ 0 & (J \ge J_{max})\,, \end{cases} \tag{9}$$

where B and a are constants and T_-^J is given by equation (6). To reproduce both A_{0n} and the observed $d\sigma/d\Omega$ for $\bar{p}p \longrightarrow \pi^-\pi^+$, we need $a \approx 0$ and $J_{max} = 4$. This is a black-sphere amplitude of radius equal to J_{max}/q. For the reaction $\bar{p}p \longrightarrow K^-K^+$, data requires that $a \approx 0.5$, corresponding to a grey sphere. This means that the lowest partial waves ($J = 0$ and 1) dominate in this reaction. As a consequence, we conclude that the $\bar{p}p \longrightarrow \pi^-\pi^+$ reaction occurs over a larger interaction volume than the $\bar{p}p \longrightarrow K^-K^+$ reaction [11]. This result lends support to the arguments based on an analogy with QED [12] that the larger the number of initial $\bar{q}q$ valence pairs, which need to be annihilated for a specific $\bar{N}N$ annihilation reaction to occur, the more central the reaction.

Since our explanation [11] of the maximal A_{0n} is based on a rather general diffractionlike picture, we expect that the maximal A_{0n} will persist as the incident $\bar{p}$ energy increases. (Judging from the success of a similar diffraction-model analysis for the $\pi N \longrightarrow \pi N$ scattering data for p_{lab} between 2 and 6 GeV/c [13], as well as in $\bar{p}p$ elastic scattering [14], our description is presumably valid in a similar energy range.) However, as will be discussed in the next section (see [15, 16]), we do expect our scheme based on the hadronic picture to break down at higher energies when the perturbative QCD regime of exclusive hadronic reactions is reached.

3. HIGH Q^2 EXCLUSIVE HADRONIC REACTIONS AT NONASYMPTOTIC ENERGIES

3.1. Introduction

In the following analysis of pQCD applied to hadronic reactions, the crucial observation is that hadrons have a geometric size (they are not pointlike) [17]. For short-distance pQCD exclusive hadronic-scattering processes, the quarks are all connected by high Q^2 gluons and all gluons and intermediate quark propagators are, therefore, far off-shell [1]. This means that the short distance amplitudes f_{SD} describing elastic πN scattering or the annihilation reaction $\bar{p}p \longrightarrow \pi^-\pi^+$ are all real and no polarization effects are expected. However, the Landshoff amplitudes f_L illustrated in Fig. 2 will contribute to the same exclusive hadronic-scattering processes [17]. In the f_L amplitudes, the hard gluons also carry high Q^2, but the two independent quark–quark scatterings can take place in two parallel scattering planes leading to the same final hadrons. The distance between these two independent quark–quark scatterings is determined by the sizes of the hadrons involved. The only requirement is that, after the hard (high Q^2) scattering, the final quarks (antiquarks) move (almost) parallel with (roughly) the same speed to be able to form the final hadrons as illustrated for $\pi N \longrightarrow \pi N$ scattering in Fig. 2. Since the two quark–quark scattering planes are separated by a transverse distance, we have, in this process, a relative orbital angular momentum that can couple to the spin, resulting in a LS amplitude for the hadronic reaction. Such an amplitude violates helicity conservation on the hadronic level [18]. In other words, since the Landshoff amplitudes contain soft QCD processes where a propagator is (almost) on-shell (Sudakov form factors), called "the Landshoff pinch" in the review by Mueller [19], the amplitudes f_L will, in general, be complex. As a consequence, we will observe polarization phenomena in hadronic reactions.

As a concrete example, let us first examine the $\bar{p}p \longrightarrow \pi^-\pi^+$ reaction, which has a large analyzing power $A_{0n} \approx 1$ for $p_{lab} \lesssim 2.2$ GeV/c [4 - 6]. If helicity is conserved on the hadronic level at very high energy, then A_{0n} should become zero at higher energies. This is correct only if the short-distance amplitude f_{SD} illustrated in Fig. 3*a* acts alone. As discussed in [15], the Landshoff amplitude f_L illustrated in Fig. 3*b* will contribute as well. Including the lowest-order radiative corrections, f_L will be of order α_s^4, like f_{SD} illustrated in Fig. 3a, but the amplitude f_L will fall off roughly like $s^{-2.85}$ with increasing energy, i.e., slower than f_{SD} in the energy range under discussion. However, the Landshoff process is even more intriguing and might show some tell-tale signals of pQCD. The modulus of the elementary quark-quark scattering amplitude itself cannot be calculated in pQCD. But, including the radiative corrections,

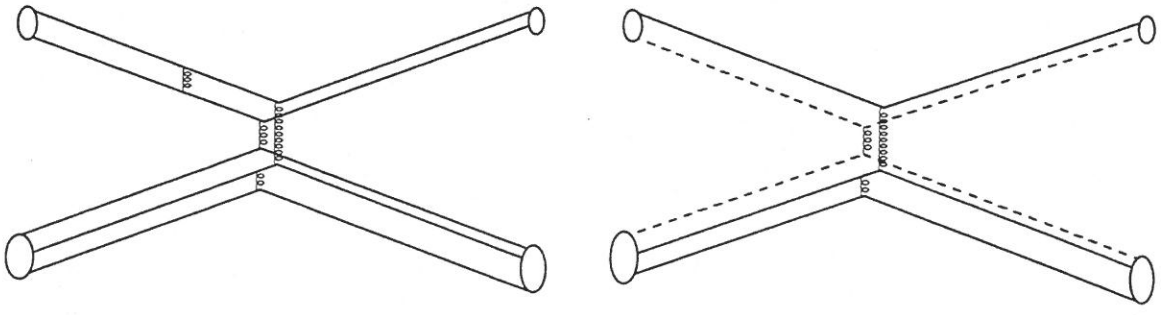

Fig. 2. Illustrations of contributions to $\pi N \longrightarrow \pi N$ scattering amplitudes. On the left is an example of a short-distance contribution to f_{SD}. On the right is a contribution to the Landshoff amplitude f_L. The dashed lines signify that this quark–quark scattering does not have to occur in the same plane as the other scattering.

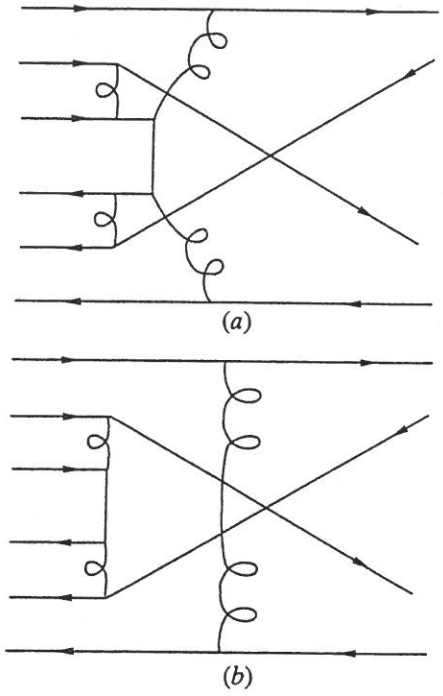

Fig. 3. (*a*) An example of a short-distance QCD diagram of order α_s^4 for the process $\bar{p}p \longrightarrow \pi\pi$. The diagram has an s^{-3} dependence. (*b*) An example of diagrams for the large-angle Landshoff process for the same reaction of order α_s^3. The timelike gluon and one quark are off-shell and the diagram gives an $s^{-5/2}$ behavior when we neglect radiative corrections.

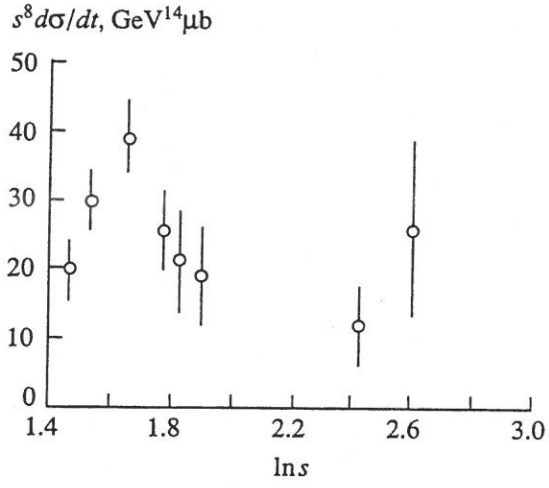

Fig. 5. The cross section for $\bar{p}p \longrightarrow \pi^-\pi^+$ at 90° scaled by s^8 as a function of ln s. Figure taken from [15].

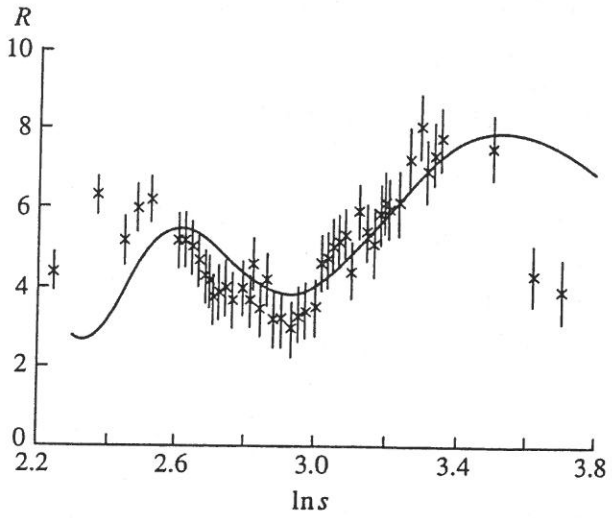

Fig. 4. The elastic pp cross section at 90° scaled by s^{10} as a function of energy. Figure taken from Carlson *et al.* [15].

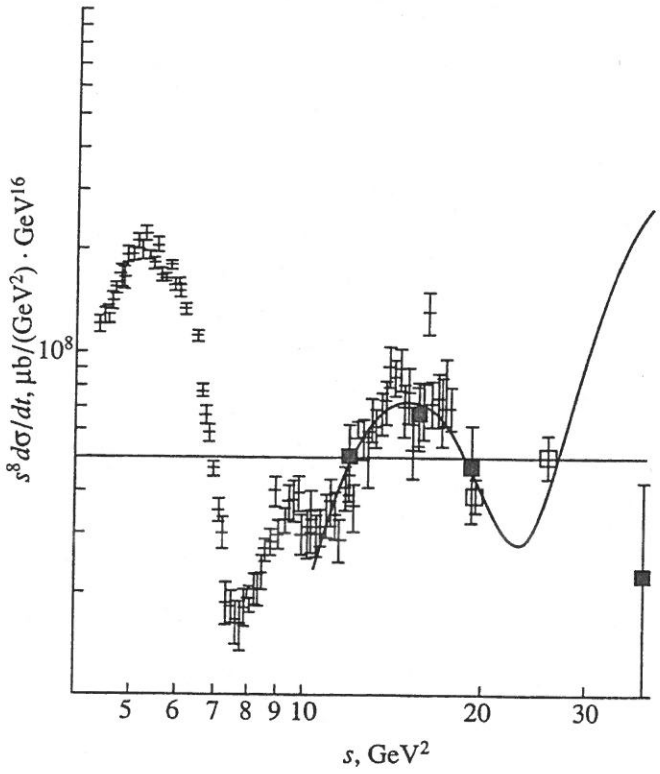

Fig. 6. The cross section for elastic $\pi N \longrightarrow \pi N$ scattering at 90° scaled by s^8. Figure taken from [28]. For s between 4 and 60 GeV^2, the differential cross section at 90° changes by 10 orders of magnitude (see [27] Fig. 23).

the f_L amplitude has an energy-dependent phase, inferred by Ralston and Pure [20], which has been calculated in perturbative QCD by Sen [21]. The analytic form of this phase is

$$\Phi \sim \frac{\pi}{6} \ln\ln(Q^2/\Lambda^2), \qquad (10)$$

where $\Lambda \approx 200$ MeV. Botts and Sterman analyzed how this phase changes in exclusive hadronic reactions and found the expression [22]

$$\Phi = a\ln\left(\frac{\ln s/\Lambda^2}{\ln 1/(b\Lambda)^2}\right) + \text{constant}, \qquad (11)$$

where we assume the constant a to be different from the perturbative QCD result of $\pi/6$ since we are not quite in the asymptotic energy region with present experimental measurements. The impact parameter b can be thought of as the average distance between the independent quark–quark scatterings discussed earlier. It has the following energy dependence [22]:

$$b\Lambda = (\sqrt{s}/\Lambda')^{-\tau}, \quad (12)$$

where $\tau \approx 0.7$ for three flavors of quarks. As discussed by Botts and Sterman [22, 23], the phase equation (11) should become independent of energy at asymptotic energies ($s \longrightarrow \infty$). In the following, we will discuss our three selected exclusive hadronic reactions.

3.2. Elastic pp Scattering

If we apply the above ideas to pp elastic scattering, we can show that not only the oscillations in the "scaled" cross section at 90° (see Fig. 4) can be reproduced, but also the spin-correlation observable A_{nn} at 90° can be described using, e.g., a value $a = 4\pi$ [15]. (In their phenomenological analysis of the "scaled" pp elastic 90° cross section, Ralston and Pire [20] needed a constant $a \approx 50$ in front of the double log to reproduce the observed period of the energy oscillations. The phenomenological arguments leading to these results follow [15]: For elastic pp scattering, the five helicity amplitudes M_i ($i = 1, ..., 5$) are of the form (the energy scale is factored out in ϕ_i)

$$\phi_i \propto s^{-4} M_i = s^{-4}\left(B_i + C_i s^{0.2} e^{i[\psi_i + \delta_i]}\right), \quad (13)$$

where the "scaled" B_i originates from the short-distance pp amplitude M_{SD}. The "scaled" amplitude C_i is the modulus of the Landshoff amplitude M_L, where the lowest-order radiative QCD correction are included. The phase of the Landshoff amplitude is deduced from equations (11) and (12) to be

$$\psi_i = a \ln\left(\frac{\ln(s/\Lambda^2)}{\ln(s/\Lambda_i^2)}\right). \quad (14)$$

In equation (13), the phase δ_i is a real constant that is possibly different for each NN helicity amplitude, and the constants Λ_i of equation (14) have values between 1.4 and 2.2 GeV to give the curve in Fig. 4 [15]. As can been seen from the above equations, we assume that the five different NN helicity amplitudes at nonasymptotic energies have slightly different energy behaviors. In our analysis, the measured, very dramatic, energy dependence of A_{nn} at 90° is understood to be a "beating" of the different energy periods in the phases of the helicity amplitudes above [15]. (For a different explanation, see [24].) With the interplay of the two amplitudes M_{SD} and M_L in equation (13), it is not difficult to reproduce the spin observables in pp elastic scattering at high Q^2. However, since pp elastic scattering has, in general, five helicity amplitudes, there is too much freedom in fitting data. Only for 90° c.m.s. scattering do the expressions simplify since $\phi_5 = 0$ and $\phi_4 = -\phi_3$, meaning, we have only three independent helicity amplitudes, which is still too many amplitudes to make a useful study of the underlying physical processes. A consequence is of course that, for pp elastic scattering at angles different from 90°, the situation is far too complex to easily learn anything about the underlying dynamic processes at high Q^2.

3.3. The Reaction $\bar{p}p \longrightarrow \pi\pi$ and πN Elastic Scattering

To examine if this phenomenological analysis is reasonable, it would be preferable to test the predictions in the two reactions $\pi N \longrightarrow \pi N$ and $\bar{p}p \longrightarrow \pi\pi$. As stated above, each of these reactions are described by only two helicity amplitudes f_{++} and f_{+-} [see equations (2) and (3)], and the cross section and the asymmetry are given by equation (1).

For the $\bar{p}p \longrightarrow \pi\pi$ reaction, the real short-distance amplitude f_{SD} contributes only to f_{+-}, whereas the Landshoff amplitude f_L contributes to both helicity amplitudes, meaning, the f_{++} amplitude will have a structure similar to (13) [15]. The energy dependences of the two amplitudes are as follows:

$$f_{SD} \propto s^{-3} \quad \text{and} \quad f_L \propto s^{-2.85}. \quad (15)$$

For these annihilation reactions, some data already exist for momenta up to $p_{lab} = 6.2$ GeV/c [25, 26]. The measured "scaled" cross sections data $s^8 d\sigma/d\Omega$ at 90° for the reaction $\bar{p}p \longrightarrow \pi^-\pi^+$ are shown in Fig. 5, taken from [15].

The elastic $\pi N \longrightarrow \pi N$ scattering cross section at 90° has been measured for momenta as high as 30 GeV/c [27]. In Fig. 6, we show the "scaled" cross section data for the $\pi N \longrightarrow \pi N$ scattering [this figure is taken from G. Blazey's thesis [28] (please ignore the curve in the figure)]. Due to the approximate s^{-8} behavior, the differential cross section at 90° changes by about 10 orders of magnitude between $s = 6$ and 60 GeV^2. Therefore, the cross section measurement at the highest energy $p_{lab} = 30$ GeV/c has uncertainties too large to be useful in this discussion and is not shown in this figure.

As is clear from Figs. 5 and 6, a few measurements at different energies with reasonable statistics are needed to establish the possible oscillatory pattern of the "scaled" cross section.

4. CONCLUSION

If the energy oscillations discussed above have anything to do with the phase $\phi(s)$ of the underlying quark–quark scattering amplitude, this oscillatory behavior should manifest itself in many exclusive hadronic reactions. The question being asked is if the "scaled" cross sections for both πN elastic scattering and the annihilation reaction $\bar{p}p \longrightarrow$ two pseudoscalar mesons do oscillate with energy similar to that observed for pp elastic scattering (see Fig. 1). If this is found to be the case, a further confirmation of the ideas presented here would be to see similar energy oscillations in A_{0n} for

the same reactions. Experimentally, since the asymmetry at low energies $p_{lab} \approx 2\text{GeV}/c$ is very large [4 - 6], the annihilation reaction $\bar{p}p \longrightarrow \pi^-\pi^+$ might be better. As discussed, we do expect the geometric hadronic impact parameter ideas used to explain this large asymmetry [11] to break down when the perturbative QCD regime of exclusive hadronic reactions is reached at higher energies [15]. The onset of the perturbative QCD regime may be signaled by a significant change in the energy and angular variation of the asymmetry. For example, the large A_{0n} at 90° and $p_{lab} \approx 2$ GeV/c will become smaller and start to oscillate with increasing energy if the QCD phenomenology outlined above is reasonable.

Judging from the oscillations of the "scaled" pp cross section of Figs. 1 and 4, and provided that these oscillations have their origin in the dynamics of quark–quark scattering as discussed here, we probably will reach energies where perturbative QCD calculations become relevant for exclusive hadronic reactions at the AGS accelerator at Brookhaven National Laboratory, at SPS at CERN, at Fermilab (E760), and at the proposed KAON facility.

ACKNOWLEDGMENTS

This work is supported in part by National Science Foundation, grant no. PHYS-9006844.

REFERENCES

1. Sivers, D., Brodsky, S.J., and Blankenbecler, R., *Phys. Rep.*, 1976, vol. 23, p. 1; Brodsky, S.J., *Proc. Workshop on Nuclear Chromodynamics*, Brodsky, S. and Moniz, E., Eds., 1986, Singapore: World Sci., p. 3.
2. Crabb, D.G. *et al.*, *Phys. Rev. Lett.*, 1990, vol. 65, p. 3241.
3. E760 Collaboration at Fermilab, J. Reid, *Doctorate Dissertation*, 1993, Penn. State Univ. (in preparation).
4. Eisenhandler, E. *et al.*, *Nucl. Phys. B*, 1975, vol. 96, p. 109; Cater, A.A. *et al.*, *Nucl. Phys. B*, 1977, vol. 127, p. 202.
5. Tessarotto, F. *et al.*, *Nucl. Phys. B*, 1989, vol. 8, p. 141.
6. Hasan, A. *et al.*, *Nucl. Phys. B*, 1992, vol. 378, p. 3.
7. Liu, G.Q. and Tabakin, F., *Phys. Rev. C: Nucl. Phys.*, 1990, vol. 41, p. 665.
8. Mull, V., Holinde, K., and Speth, J., *Jülich Preprint*, 1991, no. KFA-IKP(YH) 1991-37.
9. Carter, A.A. *et al.*, *Phys. Lett. B*, 1977, vol. 67, p. 117; Carter, A.A., *Phys. Lett. B*, 1977, vol. 67, p. 122.
10. Martin, B.R. and Oades, G.C., *Nucl. Phys. A*, 1988, vol. 483, p. 669; Isgur, N. and Königsmann, K., *Nucl. Phys. A*, 1991, vol. 527, p. 491c.
11. Takeuchi, S., Myhrer, F., and Kubodera, K., *4th Conf. on the Intersections between Particle and Nuclear Physics, AIP Conf. Proc.*, 1992, vol. 243, p. 358; *Workshop on Physics at SuperLEAR*, Inst. Phys. Conf. Ser., 1992, vol. 124, p. 303; *Nucl. Phys. A*, 1993, vol. 556, p. 601.
12. Carbonell, J. *et al.*, *Z. Phys. A: At. Nucl.*, 1989, vol. 334, p. 329.
13. Høgaasen, H., *Phys. Norv.*, 1971, vol. 5, p. 219; Høgaasen, H. and Michael, C., *Nucl. Phys. B*, 1972, vol. 44, p. 214; Barger, V. and Phillips, R.J.N., *Nucl. Phys. B*, 1975, vol. 87, p. 221.
14. Eisenhandler, E. *et al.*, *Nucl. Phys. B*, 1976, vol. 113, p. 1.
15. Carlson, C.E., Chachkhunashvili, M., and Myhrer, F., *Phys. Rev. D: Part. Fields*, 1992, vol. 46, p. 2891.
16. Myhrer, F., *Hadron Scattering and Spin Sessions at the Workshop on Future Directions in Particle and Nuclear Physics at Multi-GeV Hadron Beam Facilities*, Geesaman, D. *et al.*, Eds., 1993, Brookhaven National Laboratory.
17. Landshoff, P.V., *Phys. Rev. D: Part. Fields*, 1974, vol. 10, p. 1024.
18. Ralston, J.P. and Pire, B., *Polarized Collider Workshop*, Penn. State Univ., AIP Conf. Proc., 1992, vol. 223, p. 228; *Preprint of Univ. Kansas*, 1992, 5-15-92.
19. Mueller, A.H., *Phys. Rep.*, 1981, vol. 73, p. 237.
20. Ralston, J.P. and Pire, B., *Phys. Rev. Lett.*, 1982, vol. 49, p. 1605.
21. Sen, A., *Phys. Rev. D: Nucl. Phys.*, 1983, vol. 28, p. 860.
22. Botts, J. and Sterman, G., *Nucl. Phys. B*, 1989, vol. 325, p. 62.
23. Botts, J., *Nucl. Phys. B*, 1990, vol. 353, p. 20.
24. Brodsky, S.J. and de Teramond, G.F., *Phys. Rev. Lett.*, 1988, vol. 60, p. 1924.
25. Eide, A. *et al.*, *Nucl. Phys. B*, 1973, vol. 60, p. 173.
26. Buran, T. *et al.*, *Nucl. Phys. B*, 1976, vol. 116, p. 51.
27. Baglin, C. *et al.*, *Nucl. Phys. B*, 1983, vol. 216, p. 1.
28. Blazey, G., *Doctorate Dissertation*, 1987, Univ. Minnesota.